

Cite this: *Chem. Sci.*, 2025, 16, 20368

All publication charges for this article have been paid for by the Royal Society of Chemistry

Received 7th July 2025  
Accepted 16th September 2025

DOI: 10.1039/d5sc04998a

rsc.li/chemical-science

## Two-carbon ring expansion of bicyclic aziridines to oxazocines *via* aryne insertion into a $\sigma$ C–N bond

Daniel S. Rampon,<sup>a</sup> Tuan Anh Trinh,<sup>b</sup> Yekun Pan,<sup>a</sup> Sierra Thein,<sup>a</sup> Jacob W. Kailing,<sup>a</sup> Iliia A. Guzei,<sup>a</sup> Israel Fernández<sup>b</sup>\* and Jennifer M. Schomaker<sup>b</sup>\*

Oxazocines are medium-sized N,O-heterocycles that are motifs in reported bioactive compounds; thus, methods for their rapid preparation and functionalization are of significant interest, particularly to increase their representation in current drug libraries. In this work, a mild method to access oxazocines through aryne insertion into the  $\sigma$  C–N bond of carbamate-tethered bicyclic aziridines is described. This work unlocks a complementary reactivity mode for bicyclic aziridines *via* a two-carbon ring expansion, which preserves both the strained ring and its stereochemical information for further modifications. Mechanistic studies of the reaction pathway using Density Functional Theory computations indicate that oxazocine formation *via* nucleophilic acyl substitution of the carbonyl group of the carbamate is kinetically preferred over alternative products arising from aziridine ring-opening pathways.

### Introduction

N-Heterocycles are common motifs in pharmaceuticals, natural products, and fine chemicals, and continue to inspire the development of innovative strategies for their synthesis from versatile precursors. In fact, N-heterocycles are found as structural components in ~82% of recent U.S. FDA-approved small-molecule drugs (January 2013–December 2023), with the majority of these comprised of 5- and 6-membered rings.<sup>1</sup> In contrast, medium-sized rings (8–11-membered) are underrepresented in current drug screening libraries,<sup>1,2</sup> despite the attractive interplay between their rigidity and broad conformational space that may lead to improved binding affinity to biological receptors, oral bioavailability, and cell permeability.<sup>3</sup> In particular, natural and synthetic eight-membered N,O-heterocycles, including oxazocines, show valuable bioactivities that remain underexplored in compound screening collections, largely due to challenges inherent in their syntheses (Scheme 1A).<sup>4</sup>

Common strategies for the syntheses of substituted oxazocines include head-to-tail cyclizations, cycloadditions, ring fragmentations, ring contractions, and ring expansions (Scheme 1B).<sup>5</sup> The kinetic barriers associated with head-to-tail cyclizations are typically high due to unfavorable entropy and enthalpy contributions to the transition state in the formation of medium-sized rings.<sup>6</sup> These systems require careful optimization to prevent unwanted intermolecular reactions, such as

dimerization and oligomerization. In addition, control over the relative and absolute stereochemistry has not been addressed in the preparation of oxazocines, leading to a need for new methods to prepare the heterocycles from readily available building blocks.

The construction of eight-membered cyclic frameworks *via* ring contraction or expansion strategies circumvents many of the common challenges associated with medium-sized ring formation.<sup>7</sup> In recent years, our group has explored ring expansions of unusual aziridinium ylides, generated by the nucleophilic attack of bicyclic aziridines on metal-supported carbenes.<sup>8,9</sup> The nitrogen of the carbamate-derived bicyclic aziridine precursor displays near-sp<sup>3</sup> hybridization, which increases the nucleophilicity of the aziridine's nitrogen lone pair. Reaction with an electrophile bearing a latent nucleophile gives an intermediate with three electrophilic sites that may undergo strain-release ring-opening to enlarge the ring (Scheme 1C).<sup>8</sup> Judicious choice of substrate, catalyst and reaction conditions enable us to successfully harness the reactivity of aziridinium ylides to furnish densely substituted, stereochemically complex N-heterocycles.

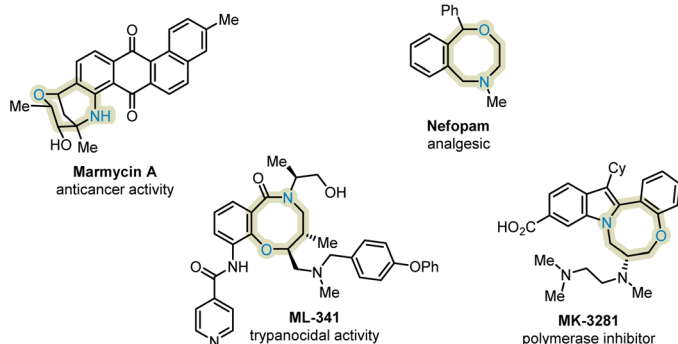
Arynes are highly reactive intermediates that function as polarized two-carbon synthons for the 1,2-difunctionalization of arenes.<sup>10</sup> The low-lying LUMO resulting from the strained nature of the C $\equiv$ C triple bond makes arynes susceptible to attack even by weak nucleophiles,<sup>11</sup> such as non-activated aziridines. Reported examples of the addition of aziridines to arynes, generated from *o*-silylaryl triflates, typically yield products from fragmentation or ring-opening of the aziridinium ion by external nucleophiles (Scheme 1D).<sup>12</sup> An exception was reported by the Studer group showing intramolecular ring expansion of vinyl aziridines in the absence of fluoride ion.<sup>12g</sup>

<sup>a</sup>Department of Chemistry, University of Wisconsin, Madison, Wisconsin 53706, USA. E-mail: schomakerj@chem.wisc.edu

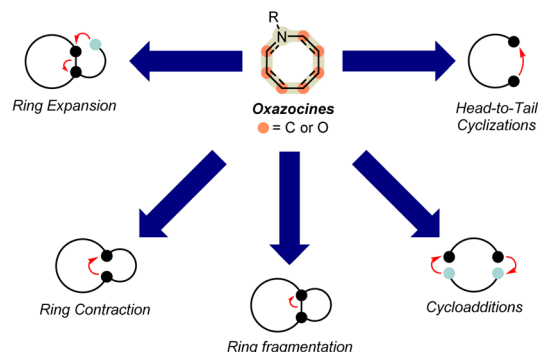
<sup>b</sup>Departamento de Química Orgánica I and Centro de Innovación en Química Avanzada (ORFEO-CINQA), Facultad de Ciencias Químicas, Universidad Complutense de Madrid, Madrid 28040, Spain. E-mail: israel@quim.ucm.es



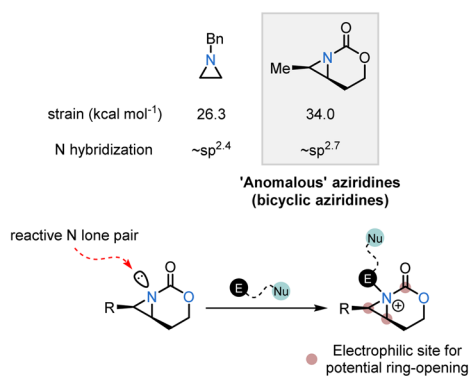
A: Selected oxazocines in natural products and drugs



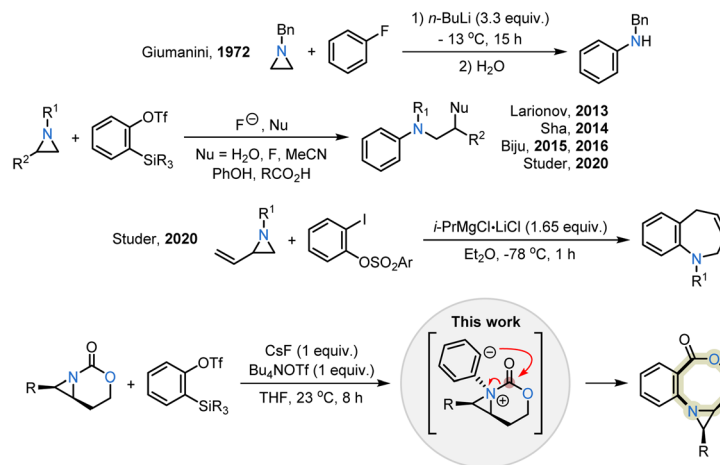
B: General strategies to access oxazocines



C: 'Anomalous' aziridines building blocks



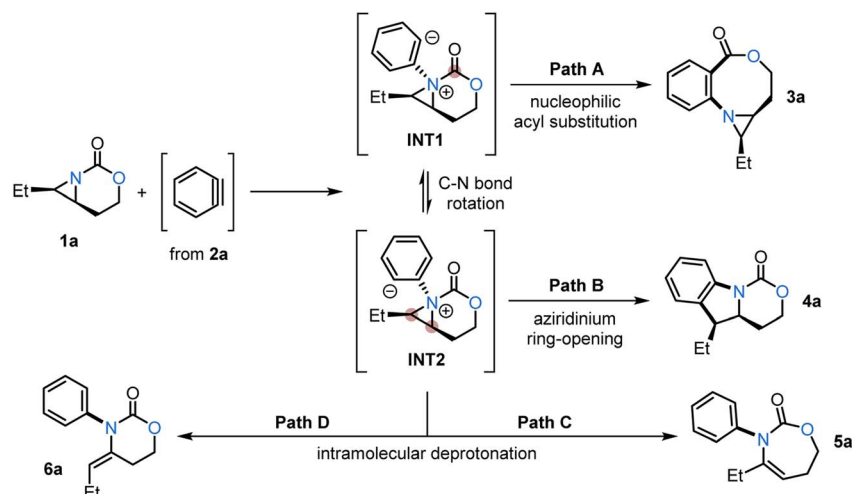
D: Reactions between aziridines and arynes



Scheme 1 (A) Selected oxazocines in natural products and drugs. (B) General strategies to access oxazocines. (C) 'Anomalous' aziridine building blocks. (D) Reactions of aziridines and arynes.

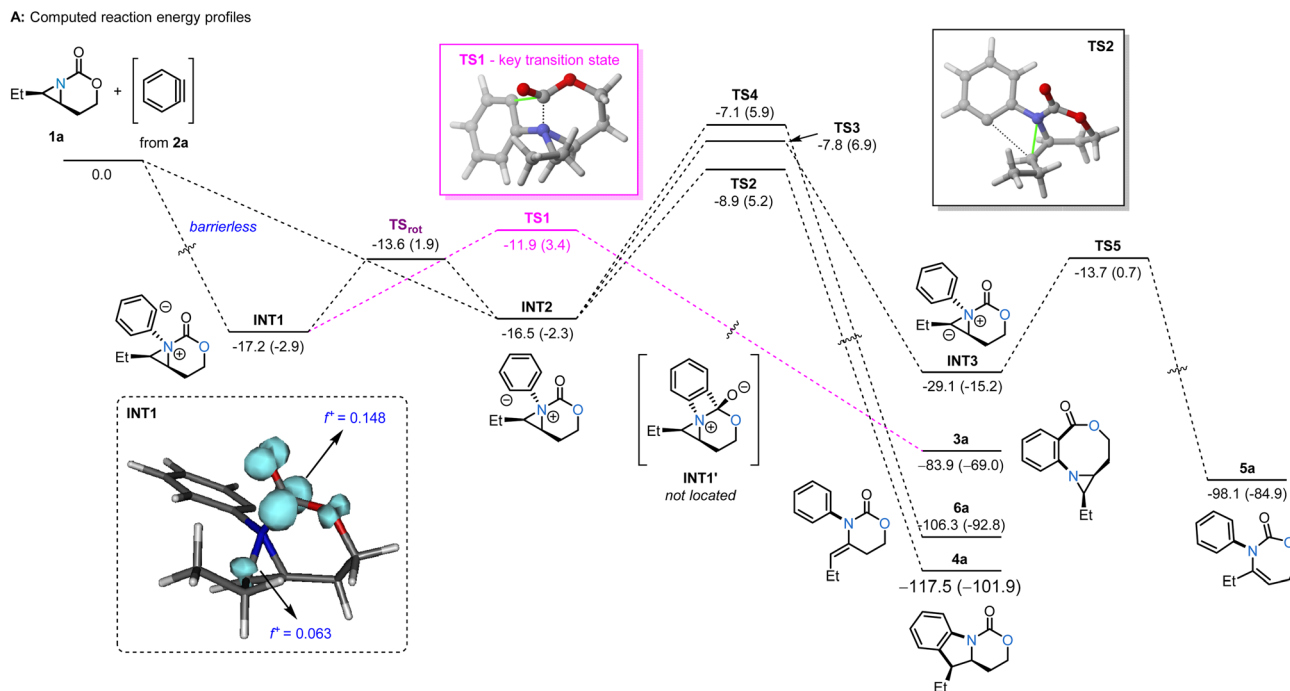
Given the unusual reactivity of carbamate-derived bicyclic aziridines, we proposed they might serve as building blocks to construct oxazocines *via* aziridinium intermediates generated from arynes. Attack of the aryne by the bicyclic aziridine

generates a highly basic, nucleophilic aryl anion intermediate that undergoes rapid intramolecular nucleophilic acyl substitution instead of the expected competing aziridine ring-opening. The insertion of the aryne into a C–N  $\sigma$ -bond

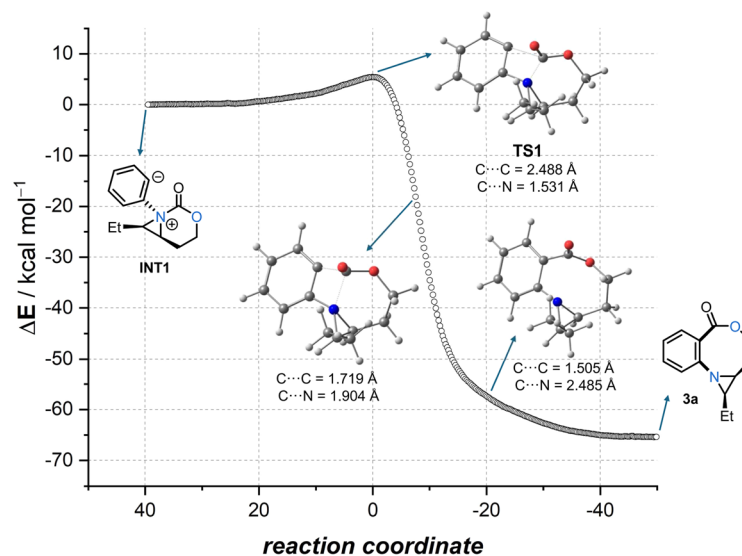


Scheme 2 Two-carbon ring expansion of 1a with benzyne to furnish 3a (Path A) and an alternative pathway to 4a (Path B), 5a (Path C) and 6a (Path D).





B: Intrinsic Reaction Coordinate (IRC) of TS1



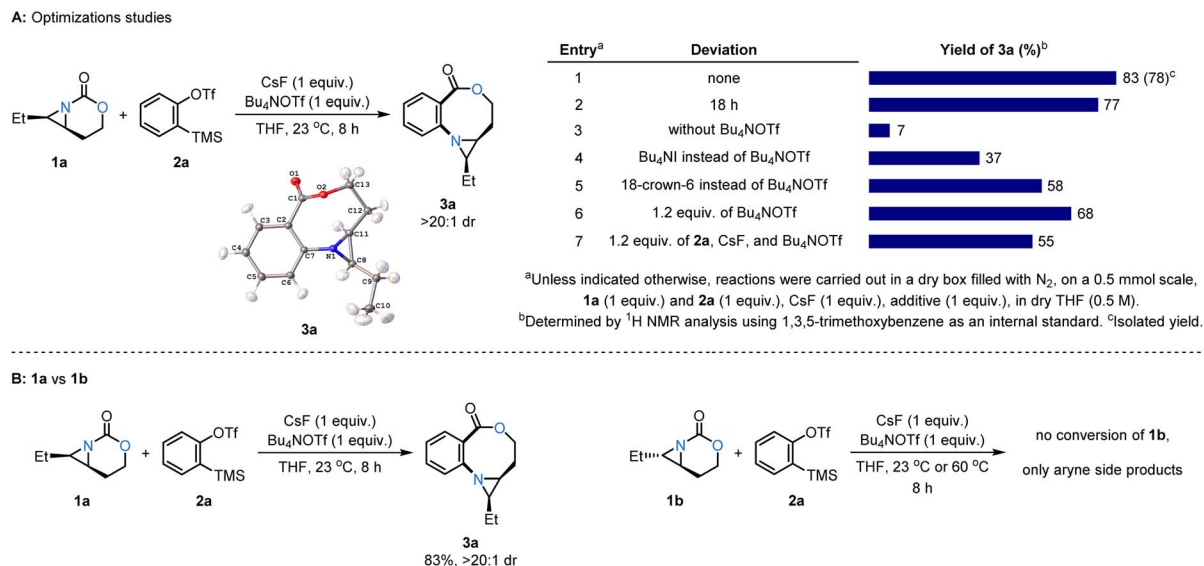
Scheme 3 (A) Computed reaction profile for the reaction between benzyne and aziridine **1a**. Relative enthalpies ( $\Delta H$ ) and free energies ( $\Delta G$ ) (within parentheses, at 298 K) are given in  $\text{kcal mol}^{-1}$ . (inset): Computed condensed Fukui functions ( $f^+$ ) in **INT1**. (B) Intrinsic reaction coordinate computed for the transformation of **INT1** into **3a**. All data have been computed at the SMD(THF)-B3LYP-D3/def2-TZVPP//SMD(THF)-B3LYP-D3/def2-SVP level.

preserves the aziridine as a useful handle for further transformations (Scheme 1D). Herein, we report the successful demonstration of this formal cut-and-sew strategy to furnish oxazocines bearing a useful fused aziridine ring. No competing intermolecular nucleophilic opening of the aziridinium ion intermediate is observed, while full transfer of stereochemical information from the precursor to the product can be harnessed for subsequent stereoselective oxazocine functionalizations.

## Results and discussion

Investigations were initiated by first assessing whether the aziridine **1a** undergoes nucleophilic addition to a benzyne formed from 2-(trimethylsilyl)phenyl triflate (**2a**). The resulting aziridinium ion intermediate (**INT1**) could furnish oxazocine **3a** (Scheme 2, Path A) by ring-opening of the carbamate. Alternatively, **INT1** could undergo C-N bond rotation to furnish conformer **INT2**; opening of the aziridine by the aryl anion





Scheme 4 (A) Optimization studies. (B) Reaction of *cis*-1a vs. *trans*-1b.

would give 4a (Scheme 2, Path B). Based on previous studies,<sup>12a</sup> intramolecular deprotonations leading to 5a or 6a are also plausible outcomes for this reaction (Scheme 2, Paths C and D).

To this end, we first computationally explored the reaction between aziridine 1a and a benzyne using Density Functional Theory (DFT) calculations at the dispersion corrected SMD(THF)-B3LYP-D3/def2-TZVPP//SMD(THF)-B3LYP-D3/def2-SVP level (Scheme 3A). Similar to related nucleophilic additions to benzyne,<sup>13</sup> the process begins with a barrierless, highly exothermic formation of INT1 or its isomer INT2 ( $\Delta H \approx -17$  kcal mol<sup>-1</sup> from the separate reactants).<sup>14</sup> Both initial intermediates are nearly degenerate ( $\Delta\Delta H = 0.7$  kcal mol<sup>-1</sup>), with INT1 being slightly more stable; conformers are easily interconverted through transition state TS<sub>rot</sub> by simple rotation along the newly formed Csp<sup>2</sup>-N bond with a low activation barrier of 3.6 kcal mol<sup>-1</sup> ( $\Delta\Delta H$ ). Interestingly, INT1 can be directly transformed into oxazocine 3a through transition state TS1, a saddle point which is mainly associated with the formation of the new Csp<sup>2</sup>-C(=O) bond with a low barrier of 5.3 kcal mol<sup>-1</sup> ( $\Delta\Delta H$ ) in a highly exothermic ( $\Delta H_R = -66.7$  kcal mol<sup>-1</sup>) reaction. Instead of forming the four-membered ring intermediate INT1', intrinsic reaction coordinate (IRC) calculations confirm that this intermediate is unstable on the potential energy surface and rapidly evolves to the oxazocine 3a (Scheme 3B), supporting that the formation of the new Csp<sup>2</sup>-C(=O) bond is also associated with the concomitant (O=C)-N bond rupture.

In contrast, INT2 can be transformed into tricyclic species 4a, which is thermodynamically more stable than 3a ( $\Delta\Delta H = -33.6$  kcal mol<sup>-1</sup>). However, the formation of 4a (via transition state TS2) requires a higher barrier of 7.6 kcal mol<sup>-1</sup> ( $\Delta\Delta H$ ), indicating that the formation of the oxazocine is kinetically favored. Similarly, the alternative intramolecular deprotonation/aziridine ring-opening processes (involving TS3 and TS4) leading to species 5a and 6a, although

thermodynamically favored over the formation of the oxazocine, also proceed with higher barriers ( $\Delta H^\ddagger = 8.7$  and 9.4 kcal mol<sup>-1</sup>, respectively). Therefore, our calculations suggest that the formation of the oxazocine is kinetically preferred over other possible reaction products. This preference likely arises from the higher electrophilicity of the carbonyl carbon atom as compared to the carbon atom of the aziridine; this was confirmed by the corresponding condensed Fukui functions ( $f^\ddagger$ ) computed at the reactive intermediate INT1 (see inset in Scheme 3).

The striking preference for formation of the oxazocine ring 3a was experimentally confirmed using 1a and the Kobayashi aryne precursor 2a, which afforded 3a as the only product in a high dr of >20:1 under several conditions (Scheme 4A). The structure of 3a was further supported by single-crystal X-ray diffraction (see Section 11 in the SI for details), where the *cis* stereochemistry of the aziridine ring was preserved during the course of the reaction. After extensive screening (see Table S1 in the SI for further details), the formation of the oxazocine 3a was found to proceed in optimal yield using CsF and Bu<sub>4</sub>NOTf as a fluoride-solubilizing agent<sup>15</sup> in THF as the solvent at room temperature (Scheme 4A, entry 1). We found that diverse commercially available sources of fluoride promoted reactivity, while other aryne sources were less efficient replacements for *o*-silylaryl triflates (see Scheme S1 in the SI for details). The *o*-silylaryl triflates were ideal precursors, as only mild conditions are required to trigger *in situ* formation of the desired aryne. Representative optimization studies show a considerably lower yield of 3a in the absence of Bu<sub>4</sub>NOTf (entry 3); other common additives to enhance the solubility of fluoride salts proved inferior compared to standard conditions (entries 4, 5). Furthermore, the yield of 3a was not improved with extended reaction time (entry 2) and only moderate yields were observed using an excess of 2a, CsF, and Bu<sub>4</sub>NOTf (entries 6, 7). Conversely, even under forcing conditions, the *trans* isomer 1b



showed no conversion to the desired oxazocine (Scheme 4B).<sup>9b</sup> As noted earlier, the *cis* isomer **1a** gives **3a** in good yield, highlighting that ready access to the nitrogen lone pair is essential for efficient reaction with the aryne.

The scope of the two-carbon ring expansion of carbamate-tethered bicyclic aziridines with diverse aryne precursors was explored (Table 1, top). Reaction of the *cis*-aziridine **1a** with **2a-p** gave the oxazocines **3a-p**, where the *cis* stereochemistry of the aziridine **1a** was conserved in the product. No competing reactions of the *cis*-bicyclic aziridines were observed; the remaining mass balance consisted of remaining **1a** and varying amounts of **2a-p**. Bicyclic aziridine **1a** was then reacted with a series of 3-substituted aryne precursors **2b-f**; the resulting products **3b-f** were obtained exclusively from the nucleophilic attack of the aziridine nitrogen at the less sterically hindered terminus on the aryne intermediate, which is also more distorted toward

linearity.<sup>16</sup> The high sensitivity of the reaction to steric effects is highlighted in reactions of 3,6-disubstituted *o*-silylaryl triflates **2g** and **2h**, which delivered low yields of the products **3g** and **3h** even under relatively harsh conditions. However, moderate-to-good yields were restored when the substituents on the Kobayashi aryne precursor were located distal to the approach trajectory between the aziridine nitrogen and the aryne, as observed for oxazocines **3i-m**. The 4-substituted aryne precursor **2l**, which bears an electron-withdrawing chlorine, provided greater regioselectivity in **3l** resulting from nucleophilic attack of the aziridine at the *para*-position as compared to **3k** (**3l**: 2.7:1 rr vs. **3k**: 1:1.3 rr).<sup>17</sup> The reaction was also successful with ring-fused-arynes, producing **3n** as the sole product in 54% yield. Benzo-fused five-membered heterocyclic aryne precursors were also compatible with this method, as exemplified by the use of **2o**, a precursor of 4,5-benzofuranyne,

Table 1 Scope of oxazocine formation with diverse *cis*-aziridines and aryne precursors

**A: *o*-Silylaryl triflates<sup>a-c</sup>**

R	Yield	<i>dr</i>
H	<b>3a</b> , 78%	20:1
OMe	<b>3b</b> , 68%	20:1
Me	<b>3c</b> , 46%	20:1
Ph	<b>3d</b> , 68%	20:1
F	<b>3e</b> , 62%	20:1
Br	<b>3f</b> , 45%	20:1

R	Yield	<i>dr</i>
OMe	<b>3g</b> , 9% <sup>d</sup> , 1% <sup>e</sup>	20:1
Me	<b>3h</b> , 7% <sup>d</sup>	20:1

R	Yield	<i>dr</i>
Me	<b>3i</b> , 65%	20:1
F	<b>3j</b> , 67%	20:1

Structure	Yield	<i>dr</i>
<b>3k</b>	61%, >20:1 <i>dr</i>	1:1.3 rr (4-Me:3-Me) <sup>f</sup>
<b>3l</b>	56%, >20:1 <i>dr</i>	2.7:1 rr (4-Cl:3-Cl) <sup>f</sup>
<b>3m</b>	73%, >20:1 <i>dr</i>	
<b>3n</b>	54%, >20:1 <i>dr</i>	
<b>3o</b>	70%, >20:1 <i>dr</i>	
<b>3p</b>	15%, >20:1 <i>dr</i>	44% <sup>g</sup> , >20:1 <i>dr</i>

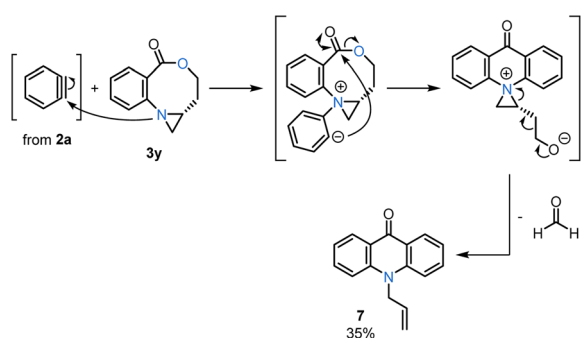
**B: Anomalous aziridines<sup>a-c</sup>**

Structure	Yield	<i>dr</i>
<b>3q</b>	51%, >20:1 <i>dr</i>	
<b>3r</b>	83%, >20:1 <i>dr</i>	
<b>3s</b>	57%, >20:1 <i>dr</i>	
<b>3t</b>	68%, >20:1 <i>dr</i>	
<b>3u</b>	77%, >20:1 <i>dr</i>	
<b>3v</b>	57%, >20:1 <i>dr</i>	
<b>3x</b>	61%, >20:1 <i>dr</i>	
<b>3y</b>	0% <sup>h</sup>	

<sup>a</sup>Conditions: Unless indicated otherwise, reactions were carried out in a dry box filled with N<sub>2</sub>, on a 0.5 mmol scale, **1a** or **1c-j** (1 equiv.) and **2a-p** (1 equiv.), CsF (1 equiv.), Bu<sub>4</sub>NOTf (1 equiv.), in dry THF (0.5 M). <sup>b</sup>Diastereomeric ratio (*dr*) values based on <sup>1</sup>H NMR analysis of crude mixtures. <sup>c</sup>Isolated yields. <sup>d</sup>24 h. <sup>e</sup>60 °C. <sup>f</sup>Regioisomeric ratio (rr) values based on <sup>1</sup>H NMR analysis of the inseparable mixture after purification. <sup>g</sup>Dry MeCN (0.5 M), 2 h, CsF (3 equiv.). <sup>h</sup>*N*-allyl acridone **7** (see SI for details) was the main isolated product in 35% yield.



which furnished a 70% yield of **3o** in a regioselectivity consistent with the aryne distortion model.<sup>18</sup> Given the importance of pyridines in medicinal chemistry, the compatibility of the reaction with a 2,3-pyridyne Kobayashi precursor **2p** was assessed. Gratifyingly, the ring expansion smoothly produced oxazocine **3p** in 44% yield after minor alterations to the standard reaction conditions;<sup>19</sup> no trace of any other regioisomers were observed. Unfortunately, all attempts to translate this chemistry into the addition of bicyclic aziridines to strained alkynes and allenes proved unsuccessful (see Fig. S1 in the SI for further details). The higher LUMO energies of strained alkynes and allenes relative to arynes, together with distinct rates of intermediate formation under the optimized conditions,<sup>20</sup> preclude productive use of other fleeting strained intermediates in this reaction.

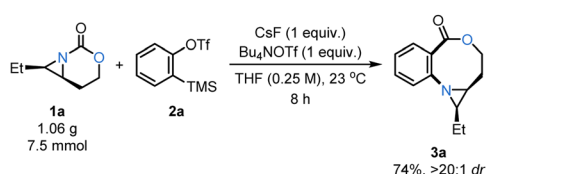


Scheme 5 Proposed mechanism for *N*-allyl acridone (**7**) formation from **3y** and **2a**.

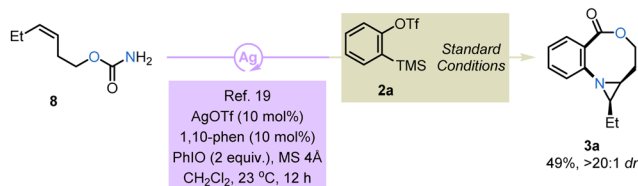
We next investigated the facility of the ring expansion with a series of *cis*-substituted bicyclic aziridines (**1c–j**) that display distinct side chains (Table 1, bottom). In general, the oxazocines **3q–y** were obtained as the sole products in good-to-moderate yields and a high dr of >20:1. Secondary, tertiary, and quaternary carbon substituents were tolerated (**3q–t**) under these mild reaction conditions, and no side products were detected from alkyl migration, elimination, or fluoride-mediated aziridinium ring opening. A bicyclic aziridine **1d**, containing an *N*-Boc protected amine, was also suitable, giving a good yield of **3r**. Another interesting feature of this chemistry was its compatibility with a *tert*-butyldiphenylsilyl (TBDPS)-protected alcohol in **1g** to furnish **3u** in 77% yield, despite the well-known use of fluoride to deprotect silyl ethers. Additionally, aziridines substituted with primary alkyl chlorides (**1h**) or ethers (**1i**) were successful reaction partners with benzyne, providing **3v** and **3x** in 57% and 61% yields, respectively. Lastly, less-substituted bicyclic aziridines also undergo this ring expansion. However, the aziridine of **3y** proved more nucleophilic than that of the **1j** precursor, leading to full consumption of the oxazocine **3y** through a second addition to benzyne. The major *N*-allyl acridone **7** product resulted from intramolecular nucleophilic acyl substitution, followed by formaldehyde extrusion (Table 1 and Scheme 5).<sup>21</sup>

To highlight the usefulness of this transformation, a gram-scale reaction was conducted with **1a** (1.06 g, 7.5 mmol) and **2a** under slightly modified conditions, with no significant loss in efficiency (Scheme 6A). Another key feature of this transformation is the ability to telescope intramolecular Ag-catalyzed

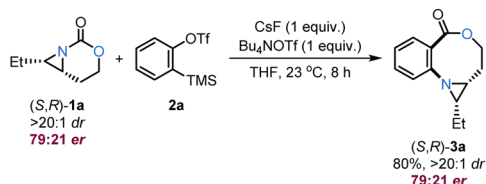
A: Gram-scale reaction<sup>a</sup>



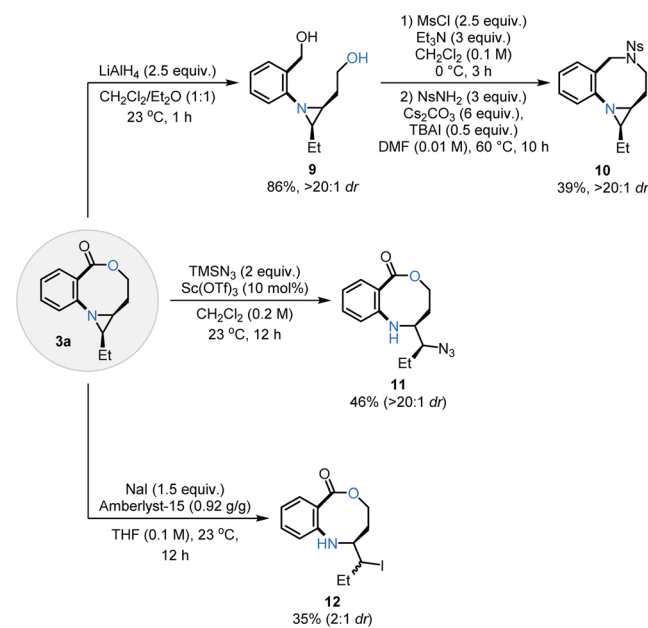
B: Telescoped intramolecular aziridination/two-carbon ring expansion<sup>b</sup>



C: Stereochemical retention experiment<sup>a</sup>



D: Synthetic applications of oxazocines<sup>a</sup>



<sup>a</sup>Isolated yields.

<sup>b</sup>Yield by <sup>1</sup>H NMR analysis using 1,3,5-trimethoxybenzene as an internal standard.

Scheme 6 Synthetic utility of two-carbon ring expansion to oxazocines. (A) Gram-scale reaction. (B) Telescoped intramolecular aziridination/two-carbon ring expansion. (C) Stereochemical retention experiment. (D) Synthetic applications of oxazocines.



nitrene transfer (NT) of the homoallylic carbamates<sup>22</sup> with the two-carbon ring expansion (Scheme 6B). After a short Celite pad and drying, the crude mixture from intramolecular aziridination of **8** was submitted to ring expansion, giving 49% of **3a** after two steps. The synthetic utility of ring expansion using arynes was enhanced by employing enantioenriched anomalous aziridines (Scheme 6C). When the enantioenriched bicyclic aziridine (*S,R*)-**1a** (79 : 21 er) was treated with **2a** under optimized conditions, complete retention of the stereochemical information at the aziridine stereocenters was observed in the resulting oxazocine **3a** (79 : 21 er, (*S,R*)-**3a**), opening a valuable path for subsequent stereoselective oxazocine functionalizations.

The oxazocine ring fused to an aziridine moiety is synthetically quite versatile, enabling chemoselective functionalization of both the oxazocine and aziridine units under mild conditions (Scheme 6D). Reduction of the ester of **3a** with LiAlH<sub>4</sub> provided the corresponding diol **9** in 86% yield,<sup>23</sup> delivering a pathway to convert the oxazocine ring into a diazocine **10** after dimesylation and dialkylation with NsNH<sub>2</sub>.<sup>24</sup> We further demonstrated that the fused aziridine ring in **3a** can be selectively opened using a combination of a Lewis or Brønsted–Lowry acid and a nucleophile. In the reaction, **3a** was treated with Sc(OTf)<sub>3</sub> and TMSN<sub>3</sub> as the azide source to give **11** in 46% yield and >20 : 1 dr.<sup>25</sup> Lastly, ring-opening with iodide and Amberlyst-15 furnished **12** in 35% yield and 2 : 1 dr.<sup>26</sup> The reaction sequences in Scheme 6 demonstrate that under controlled conditions, the stereochemical information from the anomalous aziridines can be harnessed in the oxazocine fused aziridines for the synthesis of enantioenriched medium-sized N,O-heterocycles.

## Conclusions

In conclusion, we have reported practical access to oxazocines through aryne insertion into the  $\sigma$  C–N bond of our anomalous aziridines. This work unlocked a complementary reactivity mode for anomalous bicyclic aziridines through a two-carbon ring expansion that allows the retention of the aziridine ring and its stereochemical information. Subsequently, we have leveraged the synthetic potential of this fused aziridine structure for relevant oxazocine functionalizations. Finally, our DFT computations have uncovered key insights indicating that the formation of the observed oxazocines occurs under kinetic control in view of the lower activation barrier computed for the nucleophilic substitution on the carbamate moiety as compared to alternative pathways involving aziridine ring-opening reactions.

## Author contributions

The manuscript was written through contributions of all authors. All authors have given approval to the final version of the manuscript.

## Conflicts of interest

There are no conflicts to declare.

## Data availability

The data for **3a** has been deposited with the CCDC number 2470550.<sup>27</sup>

The data supporting this article has been included as part of the SI. See DOI: <https://doi.org/10.1039/d5sc04998a>.

## Acknowledgements

J. M. S. is grateful to the National Institutes of Health (1R35GM152043-01) for financial support of this research. J. M. S. and D. S. R. are also thankful to the Paul Bender Chemistry Instrumentation Center (NMR, mass spectrometry and X-ray crystallography) in the Department of Chemistry at UW-Madison. These facilities are funded by the NSF (CHE-1048642 and CHE-2017891), NIH (1S10 OD020022-1), the Bender Fund, UW2020, and the University of Wisconsin-Madison. I. F. is grateful for financial support from grants PID2022-139318NB-I00 and RED2022-134331-T, funded by MICIU/AEI/10.13039/501100011033.

## References

- 1 C. M. Marshall, J. G. Federice, C. N. Bell, P. B. Cox and J. T. Njardarson, *J. Med. Chem.*, 2024, **67**, 11622–11655.
- 2 (a) E. Vitaku, D. T. Smith and J. T. Njardarson, *J. Med. Chem.*, 2014, **57**, 10257–10274; (b) M. M. Heravi and V. Zadsirjan, *RSC Adv.*, 2020, **10**, 44247–44311; (c) P. Bhutani, G. Joshi, N. Raja, N. Bachhav, P. K. Rajanna, H. Bhutani, A. T. Paul and R. Kumar, *J. Med. Chem.*, 2021, **64**, 2339–2381; (d) D. G. Jimenez, V. Poongavanam and J. Kihlberg, *J. Med. Chem.*, 2023, **66**, 5377–5396.
- 3 (a) K. R. Romines, K. D. Watenpaugh, P. K. Tomich, W. J. Howe, J. K. Morris, K. D. Lovasz, A. M. Mulichak, B. C. Finzel, J. C. Lynn, M.-M. Horng, F. J. Schwende, M. J. Ruwart, G. L. Zipp, K.-T. Chong, L. A. Dolak, L. N. Toth, G. M. Howard, B. D. Rush, K. F. Wilkinson, P. L. Possert, R. J. Dalga and R. R. Hinshaw, *J. Med. Chem.*, 1995, **38**, 1884–1891; (b) R. Bauer, T. Wenderski and D. Tan, *Nat. Chem. Biol.*, 2013, **9**, 21–29; (c) H. Lee, J. Kim and M. Koh, *Molecules*, 2024, **29**, 1562; (d) Y. Du, A. Semghouli, Q. Wang, H. Mei, L. Kiss, D. Baecker, V. A. Soloshonok and J. Han, *Arch. Pharm.*, 2025, **358**, e2400890.
- 4 (a) P. Alfonsi, F. Adam, A. Passard, B. Guignard, D. Sessler and M. Chauvin, *Anesthesiology*, 2004, **100**, 37–43; (b) G. D. A. Martin, L. T. Tan, P. R. Jensen, R. E. Dimayuga, C. R. Fairchild, C. Raventos-Suarez and W. Fenical, *J. Nat. Prod.*, 2007, **70**, 1406–1409; (c) J. P. Scott, M. Alam, N. Bremeyer, A. Goodyear, T. Lam, R. D. Wilson and G. Zhou, *Org. Process Res. Dev.*, 2011, **15**, 1116–1123; (d) S. Dandapani, A. R. Germain, I. Jewett, S. le Qument, J.-C. Marie, G. Muncipinto, J. R. Duvall, L. C. Carmody, J. R. Perez, J. C. Engel, J. Gut, D. Kellar, J. L. Siqueira-Neto, J. H. McKerrow, M. Kaiser, A. Rodriguez, M. A. Palmer, M. Foley, S. L. Schreiber and B. Munoz, *ACS Med. Chem. Lett.*, 2014, **5**, 149–153; (e) T. Cañeque, F. Gomes, T. T. Mai,



- G. Maestri, M. Malacria and R. Rodriguez, *Nat. Chem.*, 2015, **7**, 744–751; (f) B. Parrino, S. Cascioferro, D. Carbone, G. Cirrincione and P. Diana, *Adv. Heterocycl. Chem.*, 2020, **132**, 135–239.
- 5 (a) R. Pflantz, J. Sluiter, M. Krička, W. Saak, C. Hoenke and J. Christoffers, *Eur. J. Org. Chem.*, 2009, **2009**, 5431–5436; (b) G. Liu, W. Huang, J. Wang, X. Liu, J. Yang, Y. Zhang, Y. Geng, W. Tan and A. Zhang, *J. Med. Chem.*, 2017, **60**, 8218–8245; (c) I. J. Barve, T. U. Thikekar and C.-M. Sun, *Org. Lett.*, 2017, **19**, 2370–2373; (d) H. Lam, Z. Qureshi, M. Wegmann and M. Lautens, *Angew. Chem., Int. Ed.*, 2018, **57**, 16185–16189; (e) M. Choury, A. B. Lopes, G. Blond and M. Gulea, *Molecules*, 2020, **25**, 3147; (f) Q. Li, R. Pan, M. Wang, H. Yao and A. Lin, *Org. Lett.*, 2021, **23**, 2292–2297; (g) N. Kaur, *8-Membered Heterocycle Synthesis*, Elsevier, Amsterdam, 1st edn, 2023; (h) L. Yin, Z. Zhang, S. Huang, Z. Wang and C. Huang, *J. Org. Chem.*, 2024, **89**, 13629–13640; (i) J. Li, Z. Dong and C. Zhao, *New J. Chem.*, 2024, **48**, 4645–4669; (j) Q. Meng, Y. Meng, Q. Liu, B. Yu, Z.-J. Li, E.-Q. Li and J. Zhang, *Adv. Sci.*, 2024, **11**, 2402170.
- 6 (a) G. Illuminati and L. Mandolini, *Acc. Chem. Res.*, 1981, **14**, 95–102; (b) G. A. Molander, *Acc. Chem. Res.*, 1998, **31**, 603–609; (c) Y.-J. Hu, L.-X. Li, J.-C. Han, L. Min and C.-C. Li, *Chem. Rev.*, 2020, **120**, 5910–5953.
- 7 (a) C. J. Roxburgh, *Tetrahedron*, 1993, **49**, 10749–10784; (b) J. R. Donald and W. P. Unsworth, *Chem.–Eur. J.*, 2017, **23**, 8780–8799; (c) T. C. Stephens and W. P. Unsworth, *Synlett*, 2020, **31**, 133–146; (d) A. K. Clarke and W. P. Unsworth, *Chem. Sci.*, 2020, **11**, 2876–2881; (e) J. M. Wootton, J. K. F. Tam and W. P. Unsworth, *Chem. Commun.*, 2024, **60**, 4999–5009.
- 8 E. T. Marris, D. S. Rampon and J. M. Schomaker, *Acc. Chem. Res.*, 2025, **58**, 231–249.
- 9 (a) K. A. Nicastrì, S. A. Zappia, J. C. Pratt, J. M. Duncan, I. A. Guzei, I. Fernández and J. M. Schomaker, *ACS Catal.*, 2022, **12**, 1572–1580; (b) S. C. Schmid, I. A. Guzei, I. Fernández and J. M. Schomaker, *ACS Catal.*, 2018, **8**, 7907–7914; (c) H. J. Dequina, J. Eshon, S. C. Schmid, W. T. Raskopf, K. M. Sanders, I. Fernández and J. M. Schomaker, *J. Org. Chem.*, 2022, **87**, 10902–10907; (d) J. Eshon, K. A. Nicastrì, S. C. Schmid, W. T. Raskopf, I. A. Guzei, I. Fernández and J. M. Schomaker, *Nat. Commun.*, 2020, **11**, 1273.
- 10 (a) J. Shi, L. Li and Y. Li, *Chem. Rev.*, 2021, **121**, 3892–4044; (b) M. Sarmah, A. Sharma and P. Gogoi, *Org. Biomol. Chem.*, 2021, **19**, 722–737; (c) H. Yoshida, *Comprehensive Aryne Synthetic Chemistry*, Elsevier, Amsterdam, 2022; (d) N. Kim, M. Choi, S.-E. Suh and D. M. Chenoweth, *Chem. Rev.*, 2024, **124**, 11435–11522.
- 11 J. M. Medina, J. L. Mackey, N. K. Garg and K. N. Houk, *J. Am. Chem. Soc.*, 2016, **138**, 10402–10405.
- 12 (a) A. G. Giumanini, *J. Org. Chem.*, 1972, **37**, 513–514; (b) D. Stephens, Y. Zhang, M. Cormier, G. Chavez, H. Armata and O. V. Larionov, *Chem. Commun.*, 2013, **49**, 6558–6560; (c) C.-Y. Tang, G. Wang, X.-Y. Yang, X.-Y. Wu and F. Sha, *Tetrahedron Lett.*, 2014, **55**, 6447–6450; (d) T. Roy, D. R. Bavisar and A. T. Biju, *J. Org. Chem.*, 2015, **80**, 11131–11137; (e) T. Roy, M. Thangaraj, R. G. Gonnadeb and A. T. Biju, *Chem. Commun.*, 2016, **52**, 9044–9047; (f) T. Roy, S. S. Bhojgude, T. Kaicharla, M. Thangaraj, B. Garaib and A. T. Biju, *Org. Chem. Front.*, 2016, **3**, 71–76; (g) S. J. Kaldas, E. Kran, C. Mück-Lichtenfeld, A. K. Yudin and A. Studer, *Chem.–Eur. J.*, 2020, **26**, 1501–1505.
- 13 (a) S. Arora, J. Zhang, V. Pogula and T. R. Hoye, *Chem. Sci.*, 2019, **10**, 9069–9076; (b) Y. Shiratori, J. Jiang, K. Kubota, S. Maeda and H. Ito, *J. Am. Chem. Soc.*, 2024, **146**, 1765–1770.
- 14 The barrierless nature of this initial nucleophilic addition is confirmed by relaxed-scans calculations, see SI.
- 15 (a) L. A. Carpino and A. C. Sau, *J. Chem. Soc. Chem. Commun.*, 1979, 514–515; (b) A. V. Kellegan, A. S. Bulger, D. C. Witkowski and N. K. Garg, *Nature*, 2023, **618**, 748–754.
- 16 (a) J. M. Medina, J. L. Mackey, N. K. Garg and K. N. Houk, *J. Am. Chem. Soc.*, 2014, **136**, 15798–15805; (b) F. M. Bickelhaupt and K. N. Houk, *Angew. Chem., Int. Ed.*, 2017, **56**, 10070–10086; (c) S. M. Bronner, J. L. Mackey, K. N. Houk and N. K. Garg, *J. Am. Chem. Soc.*, 2012, **134**, 13966–13969.
- 17 (a) H. Yoshida, in *Comprehensive Organic Synthesis*, ed. P. Knochel and G. A. Molander, Elsevier, Amsterdam, 2nd edn, 2014, pp. 517–575; (b) U. N. Rao, J. Maguire and E. Biehl, *ARKIVOC*, 2004, (i), 88–100.
- 18 T. K. Shah, J. M. Medina and N. K. Garg, *J. Am. Chem. Soc.*, 2016, **138**, 4948–4954.
- 19 (a) A. E. Goetz, T. K. Shaha and N. K. Garg, *Chem. Commun.*, 2015, **51**, 34–45; (b) J. M. Medina, M. K. Jackl, R. B. Susick and N. K. Garg, *Tetrahedron*, 2016, **72**, 3629–3634.
- 20 M. Ramirez, E. R. Darzi, J. S. Donaldson, K. N. Houk and N. K. Garg, *Angew. Chem., Int. Ed.*, 2021, **60**, 18201–18208.
- 21 (a) Y. Fang, D. C. Rogness, R. C. Larock and F. Shi, *J. Org. Chem.*, 2012, **77**, 6262–6270; (b) J. Kim and B. M. Stoltz, *Tetrahedron Lett.*, 2012, **53**, 4994–4996.
- 22 (a) J. W. Rigoli, C. D. Weatherly, J. M. Alderson, B. T. Vo and J. M. Schomaker, *J. Am. Chem. Soc.*, 2013, **135**, 17238–17241; (b) R. M. Ward, Y. Hu, N. P. Tu and J. M. Schomaker, *ChemSusChem*, 2024, **17**, e202300964.
- 23 Q. Wu, Z. Zhang, Q. Chong and F. Meng, *Angew. Chem., Int. Ed.*, 2025, **64**, e202416524.
- 24 N. Shimada, Y. Abe, S. Yokoshima and T. Fukuyama, *Angew. Chem., Int. Ed.*, 2012, **51**, 11824–11826.
- 25 T. Deng, W. Mazumdar, Y. Yoshinaga, P. B. Patel, D. Malo, T. Malo, D. J. Wink and T. G. Driver, *J. Am. Chem. Soc.*, 2021, **143**, 19149–19159.
- 26 M. Ju, C. D. Weatherly, I. A. Guzei and J. M. Schomaker, *Angew. Chem., Int. Ed.*, 2017, **56**, 9944–9948.
- 27 D. S. Rampon, T. A. Trinh, Y. Pan, S. Thein, J. W. Kailing, I. A. Guzei, I. Fernández and J. M. Schomaker, CCDC 2000643: Experimental Crystal Structure Determination, 2025, DOI: [10.5517/ccdc.csd.cc2nxt5l](https://doi.org/10.5517/ccdc.csd.cc2nxt5l).

